Atmospheric
Chemistry
and Physics

Open Access

A critical evaluation of proxy methods used to estimate the acidity of atmospheric particles

C. J. Hennigan[1], J. Izumi[1], A. P. Sullivan[2], R. J. Weber[3], and A. Nenes[3,4,5]

[1]Department of Chemical, Biochemical and Environmental Engineering, University of Maryland, Baltimore County, Baltimore, MD, USA
[2]Department of Atmospheric Science, Colorado State University, Fort Collins, CO, USA
[3]School of Earth and Atmospheric Sciences, Georgia Institute of Technology, Atlanta, GA, USA
[4]School of Chemical and Biomolecular Engineering, Georgia Institute of Technology, Atlanta, GA, USA
[5]Foundation for Research and Technology – Hellas, Patras, Greece

Correspondence to: C. J. Hennigan (hennigan@umbc.edu)

Abstract. Given significant challenges with available measurements of aerosol acidity, proxy methods are frequently used to estimate the acidity of atmospheric particles. In this study, four of the most common aerosol acidity proxies are evaluated and compared: (1) the ion balance method, (2) the molar ratio method, (3) thermodynamic equilibrium models, and (4) the phase partitioning of ammonia. All methods are evaluated against predictions of thermodynamic models and against direct observations of aerosol–gas equilibrium partitioning acquired in Mexico City during the Megacity Initiative: Local and Global Research Objectives (MILAGRO) study. The ion balance and molar ratio methods assume that any deficit in inorganic cations relative to anions is due to the presence of H^+ and that a higher H^+ loading and lower cation / anion ratio both correspond to increasingly acidic particles (i.e., lower pH). Based on the MILAGRO measurements, no correlation is observed between H^+ levels inferred with the ion balance and aerosol pH predicted by the thermodynamic models and NH_3–NH_4^+ partitioning. Similarly, no relationship is observed between the cation / anion molar ratio and predicted aerosol pH. Using only measured aerosol chemical composition as inputs without any constraint for the gas phase, the E-AIM (Extended Aerosol Inorganics Model) and ISORROPIA-II thermodynamic equilibrium models tend to predict aerosol pH levels that are inconsistent with the observed NH_3–NH_4^+ partitioning. The modeled pH values from both E-AIM and ISORROPIA-II run with gas + aerosol inputs agreed well with the aerosol pH predicted by the phase partitioning of ammonia. It appears that (1) thermodynamic models constrained by gas + aerosol measurements and (2) the phase partitioning of ammonia provide the best available predictions of aerosol pH. Furthermore, neither the ion balance nor the molar ratio can be used as surrogates for aerosol pH, and previously published studies with conclusions based on such acidity proxies may need to be reevaluated. Given the significance of acidity for chemical processes in the atmosphere, the implications of this study are important and far reaching.

1 Introduction

The acidity of atmospheric particles is a critical parameter that affects air quality and the health of aquatic and terrestrial ecosystems. Acute and chronic exposures to acidic particles have been linked to deleterious effects in people, although the underlying physiological mechanisms are unclear (Gwynn et al., 2000; Dockery et al., 1996). The deposition of acidic gases and particles has been known for decades to damage freshwater and terrestrial ecosystems (Schindler, 1988; Johnson et al., 2008). While the trends in emissions are promising in the US and western Europe, ecosystem recovery from the effects of acid deposition is a slow process that can take decades (Likens et al., 1996; Stoddard et al., 1999). This may be a source of emerging environmental crisis in places such as China, where acid deposition is increas-

ing due to rapid industrialization (Pan et al., 2013; Cao et al., 2013). Particle acidity also affects global biogeochemical cycles by controlling the solubility – and thus bioavailability – of limiting nutrients that are delivered through atmospheric deposition in many marine environments (Meskhidze et al., 2003, 2005; Nenes et al., 2011). This has important implications for marine primary productivity, the carbon cycle, and even climate (Mahowald, 2011).

Particle acidity is also a critical factor that influences many chemical processes in the atmosphere. The oxidation of S(IV) to S(VI) in liquid water, the primary pathway of sulfate formation, is highly sensitive to pH (Chameides, 1984). Halogen chemistry is strongly influenced by particle acidity, which has direct implications for the oxidation of volatile organic compounds (VOCs) and ozone formation in marine and coastal regions (e.g., Keene et al., 1998; Sander and Crutzen, 1996; Pszenny et al., 2004). Recent evidence has demonstrated that aerosol pH is also a critical parameter influencing halogen chemistry in continental locations (Brown et al., 2013; Thornton et al., 2010; Young et al., 2013). Further, aerosol acidity directly affects the deposition and lifetime of many compounds in the atmosphere through its influence on the gas–particle partitioning of semi-volatile species, including ammonia (NH_3), nitric acid (HNO_3), and organic acids (Ahrens et al., 2012; Keene et al., 2004). Aerosol acidity may affect secondary organic aerosol (SOA) formation, as well (e.g., Gaston et al., 2014; Surratt et al., 2007), although the atmospheric importance of this phenomenon remains highly uncertain (Peltier et al., 2007; Takahama et al., 2006; Tanner et al., 2009; Zhang et al., 2007; Xu et al., 2015).

Despite its significance, aerosol acidity remains very poorly constrained in the atmosphere (Keene et al., 1998). All direct measurements employ filter sampling (e.g., Jang et al., 2008; Keene et al., 2002; Koutrakis et al., 1988), which is both labor intensive and limited by poor time resolution. Measurements are also challenged by the non-conservative nature of H^+: due to buffering effects and the partial dissociation of weak acids, H^+ concentrations do not scale in proportion to the level of dilution (e.g., in aqueous filter extracts). Certain methods are also susceptible to sampling artifacts, which can greatly increase the uncertainty of an inherently challenging measurement (Pathak et al., 2004). Due to these limitations, indirect methods are frequently employed to estimate the acidity of atmospheric particles. These methods include (1) the ion balance method, (2) the molar ratio, (3) thermodynamic equilibrium models, and (4) the phase partitioning of semi-volatile species (HCl, NH_3, HNO_3). The purpose of this study is to evaluate and compare the proxy methods most commonly used to estimate aerosol acidity.

2   Methods to infer pH

Before proceeding with this analysis, it is necessary to define the different physical quantities commonly described by the term "aerosol acidity". First, it is used to represent the pH of an aerosol particle or distribution. The pH represents the hydrogen ion activity in an aqueous solution (Stumm and Morgan, 1996):

$$pH = -\log(\gamma \cdot x_{H^+}), \tag{1}$$

where γ is the hydrogen ion activity coefficient and x_{H^+} is the aqueous mole fraction of dissociated H^+. The presence of aerosol water is implicit in this definition since free H^+ cannot exist in solid particles. Second, "aerosol acidity" is commonly used to describe the loading of protons in atmospheric particles, in units of nmol m^{-3} or neq m^{-3}. This definition can take several forms, including aerosol strong acidity (H^+ contributed by strong acids that dissociate completely at most pH levels), free acidity (dissociated H^+), or total acidity (includes free H^+ and the undissociated H^+ bound to weak acids), typically defined by the measurement approach (Keene et al., 2004; Lawrence and Koutrakis, 1996). The major difference between aerosol pH and the proton loading is that pH is the H^+ concentration per liquid water volume (i.e., aerosol water) while the aerosol proton loading is the H^+ concentration per unit volume of air. Aerosol pH is the parameter of interest for the atmospheric phenomena described above, but the proton loading is often treated as a surrogate for pH. This is a critical distinction that will be discussed in detail below, especially in relation to the appropriate use of each parameter for the analysis of chemical processes in the atmosphere.

2.1   Ion balance method

The ion balance method is commonly employed to estimate the proton loading in atmospheric particles. This method is based upon the principle of electroneutrality and assumes that any deficit in measured cationic charge compared to measured anionic charge is due to the presence of protons, according to

$$[H^+] = \sum n_i [anion_i] - \sum n_i [cation_i], \tag{2}$$

where n_i is the charge of species, i, and [$anion_i$] and [$cation_i$] are the molar concentrations of anion and cation species, respectively. If the sum of measured cations exceeds that of the measured anions, then the difference is attributed to OH^-. H^+ levels under an anion deficit are then calculated from the inferred [OH^-] using the water dissociation constant, K_W. Most applications of the ion balance use inorganic ions only, even though organic acids can be important to the interpretation of aerosol acidity in diverse locations (Lawrence and Koutrakis, 1996; Metzger et al., 2006; Trebs et al., 2005), especially at relatively low acidities where organic acids dissociate and contribute to the ion balance. Neglecting this effect will lead to biases in the inferred H^+. Organic compounds can also form salt complexes with inorganic species (e.g., ammonium oxalate) (Reid et al., 1998; Paciga et al., 2014), further indicating the importance of organic acids in the ion balance.

2.2 Molar ratio

While the ion balance method is used to estimate the absolute proton loading in atmospheric particles, the molar ratio is independent of absolute concentrations. The molar ratio is a ratio of the total molar concentration of measured inorganic cations to the measured inorganic anions:

$$\text{molar ratio} = \sum(\text{cations})/\sum(\text{anions}). \tag{3}$$

It is also frequently employed as an equivalence (charge) ratio. The concept was first introduced in thermodynamic models to define major ions and composition domains (e.g., Pilinis and Seinfeld, 1987; Nenes et al., 1998; Kim et al., 1993; Fountoukis and Nenes, 2007), but never to infer the levels of acidity and pH. Thermodynamic models using the major species/composition domain approach (e.g., Fountoukis and Nenes, 2007) consider the possibility that aerosol species may volatilize enough to affect the ratio at equilibrium. Furthermore, the degree of dissociation of species such as $H_2SO_4 / HSO_4^- / SO_4^{2-}$, HNO_3 / NO_3^-, HCl / Cl^-, and NH_3 / NH_4^+ can affect the value of the ratio. In subsequent studies, however, the molar ratio has been treated as a proxy for acidity, with lower ratios corresponding to particles with the highest levels of acidity (lowest pH) (e.g., Kerminen et al., 2001). Molar ratios that yield a charge balance (i.e., equivalence ratios of unity or greater) are assumed for fully neutralized aerosol. Two common simplifications of the molar ratio approach are often applied when the concentrations of crustal elements are relatively low (e.g., Zhang et al., 2007):

$$\text{molar ratio} = NH_4^+/(Cl^- + NO_3^- + 2{}^*SO_4^{2-}) \tag{4}$$

and (e.g., Peltier et al., 2007; Tanner et al., 2009; Froyd et al., 2010):

$$\text{molar ratio} = NH_4^+/(2{}^*SO_4^{2-}). \tag{5}$$

2.3 Thermodynamic equilibrium models

Multiple thermodynamic equilibrium models have been developed to predict the behavior – most commonly the phase partitioning, liquid water content, and chemical speciation – of inorganic aerosol precursors. Previous studies have performed detailed comparisons and have explored the causes of disagreement among different thermodynamic equilibrium models (Ansari and Pandis, 1999; Zhang et al., 2000). We do not attempt to repeat this exercise. Instead, thermodynamic models are considered as one method to estimate the acidity of atmospheric particles. Two models are used in the present analysis: ISORROPIA-II (Fountoukis and Nenes, 2007; Nenes et al., 1999) and the Extended Aerosol Inorganics Model (E-AIM) (Clegg et al., 1998, 2003; Wexler and Clegg, 2002). ISORROPIA-II was designed with high computational efficiency to facilitate its incorporation in large-scale models and has seen wide usage. E-AIM is computationally expensive but is considered the benchmark since it employs few assumptions in its calculation of aerosol inorganic behavior (Zaveri et al., 2008).

Two applications of each model are considered (Fountoukis et al., 2009): (a) "forward" (or "closed") mode calculations, in which inputs to the model include T, relative humidity (RH), and the total (gas + aerosol) concentrations of aerosol precursors in the air parcel, and, (b) "reverse" (or "open") calculations, in which inputs to the model include T, RH, and the concentration of aerosol species. The output of both calculations is the concentration of species in the gas and aerosol (solid/liquid) phases, pH, and aerosol water. Highly time-resolved measurements of aerosol composition (e.g., via PILS-IC or AMS) are frequently conducted without the corresponding gas-phase aerosol precursor measurements (HCl, HNO_3, NH_3). Under this condition, it is conceptually straightforward to run the thermodynamic models in reverse mode, and this approach is frequently applied to analyze ambient and experimental data. In this analysis, we consider aerosol acidity predictions using both methods.

2.4 Phase partitioning

Aerosol pH can also be estimated from the phase partitioning of certain semi-volatile compounds, such as HNO_3 / NO_3^-, NH_3 / NH_4^+, and HCl / Cl^- (e.g., Keene et al., 2004; Meskhidze et al., 2003). The H^+ concentration in aqueous particles can be calculated assuming that the system is in equilibrium (using NH_3 / NH_4^+ as an example):

$$NH_3(g) \leftrightarrow NH_3(aq) \qquad K_H, \tag{R1}$$

$$NH_3(aq) + H_2O \leftrightarrow NH_4^+ + OH^- \qquad K_b. \tag{R2}$$
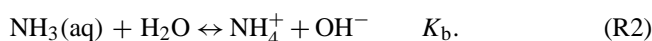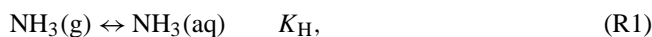
Under this approach, both the gas-phase and aerosol ionic components are measured, and the liquid H^+ concentration can be calculated after combining the equilibrium expressions from Reactions (R1) and (R2):

$$\{H^+\} = \frac{K_w\{NH_4^+\}}{K_H K_b p_{NH_3}}, \tag{6}$$

where $\{H^+\}$ is the activity of H^+ in atmospheric particles, K_H is the temperature-dependent Henry's law constant, K_b is the temperature-dependent base dissociation constant, K_w is the temperature-dependent water dissociation constant, p_{NH_3} is the gas-phase partial pressure of ammonia, and $\{NH_4^+\}$ is the activity of aqueous aerosol ammonium. The aerosol liquid water content is required to derive $\{NH_4^+\}$ (e.g., to convert from $\mu g\,m^{-3}$ to $mol\,L^{-1}$). The H^+ and NH_4^+ activity coefficients can also be calculated from thermodynamic equilibrium models in order to convert concentrations to activities, although the simplifying assumption of $\gamma = 1$ is sometimes employed, with satisfactory results (Fountoukis and Nenes, 2007).

Table 1. Overview of MILAGRO measurements used as modeling inputs.

	Measurement overview				
Species	Measurement dates (2006)	Study n	Mean concentration $\pm$ 1σ (μg m^{-3})	5th percentile (μg m^{-3})	95th percentile (μg m^{-3})
Na$^+$	10 Mar–1 Apr	998	0.31 $\pm$ 0.14	0.18	0.45
NH$_4^+$	10 Mar–1 Apr	1159	1.69 $\pm$ 1.36	0.25	4.43
Ca^{2+}	10 Mar–1 Apr	1654	0.53 $\pm$ 0.57	0.02[b]	1.64
Mg^{2+}	10 Mar–1 Apr	1051	0.15 $\pm$ 0.07	0.08	0.28
Cl$^-$	10 Mar–1 Apr	1603	0.27 $\pm$ 0.69	0.02[b]	1.23
NO$_3^-$	10 Mar–1 Apr	1634	2.93 $\pm$ 2.66	0.37	8.20
SO$_4^{2-}$	10 Mar–1 Apr	1652	3.74 $\pm$ 2.30	1.63	8.05
NH$_3$[a]	21 Mar–31 Mar	9594	25.2 $\pm$ 15.3	7.9	56.1
HNO$_3$[a]	17 Mar–30 Mar	430	2.43 $\pm$ 1.48	0.71	5.11

[a] Concentrations in ppb.
[b] This value represents the measurement limit of detection (LOD).

Table 2. Overview of modeling outputs and criteria.

|	Modeling overview				
Model	n	Average [H$^+$] (nmol m^{-3})	Median [H$^+$] (nmol m^{-3})	Average pH	Median pH
ISORROPIA-II, reverse[1]	438	19.39	10.34	1.98	-0.02
E-AIM, reverse[1]	460	15.77	6.56	2.36	0.14
ISORROPIA-II, forward[2]	89	0.008	0.005	3.31	3.38
E-AIM, forward[2]	39	0.015	0.012	3.24	3.32

[1] Output limited to samples meeting these criteria: (1) NH$_4^+$, NO$_3^-$, and SO$_4^{2-}$ >0; (2) RH $\geq$ 40 %; and (3) modeled aerosol liquid water content >0.
[2] Output limited to samples meeting these criteria: (1) NH$_4^+$, NO$_3^-$, SO$_4^{2-}$, NH$_3$, and HNO$_3$ >0; (2) RH $\geq$ 40 %; and (3) modeled aerosol liquid water content >0.

2.5 Evaluation data set

We evaluate the above methods using ground-based data collected during the Megacity Initiative: Local and Global Research Objectives (MILAGRO) campaign at the T1 site in Mexico City (Molina et al., 2010). The measurements spanned 10 March–1 April 2006 (Table 1). Inorganic PM$_{2.5}$ composition (Na$^+$, NH$_4^+$, K$^+$, Mg^{2+}, Ca^{2+}, Cl$^-$, NO$_3^-$, and SO$_4^{2-}$) was measured with a Particle-into-Liquid Sampler coupled to a dual ion chromatograph (Hennigan et al., 2008). Six-minute integrated measurements were conducted every 15 min. Given that PM$_{2.5}$ composition only was measured, no size–acidity dependence could be elucidated (Keene et al., 2002). Ammonia was measured with a quantum cascade laser spectrometer with 1 min sample time resolution (Aerodyne Research, Inc.). Nitric acid was measured with 5 min time resolution via thermal-dissociation laser-induced fluorescence of nitrogen oxides (Day et al., 2002; Farmer et al., 2011). All chloride was assumed to reside in the particle phase (i.e., gas-phase HCl was effectively 0), which was de-

termined to be a valid assumption given the high concentrations of gas-phase NH$_3$ (Fountoukis et al., 2009).

The chemical measurements, along with ambient temperature and RH, were used as inputs into ISORROPIA-II and E-AIM. Fountoukis et al. (2009) evaluated the equilibrium partitioning of semi-volatile compounds at T1 using ISORROPIA-II. We do not duplicate that effort here: instead, we focus solely on particle acidity and the comparison across the different proxy methods described above. For the reverse model runs, the 1 min met data were averaged to the aerosol sampling times and were used in conjunction with the aerosol concentrations as model inputs. Given the differences in sample timing, the forward model runs used as inputs the total gas + aerosol concentrations and met data averaged to common 10 min sample times. Output from the reverse model runs was used for the present analysis only if the following criteria were met for a given sample: (1) NH$_4^+$, NO$_3^-$, and SO$_4^{2-}$ aerosol measurements were operational; (2) RH > 40 %; and (3) modeled aerosol liquid water > 0. Output from the forward model runs was used
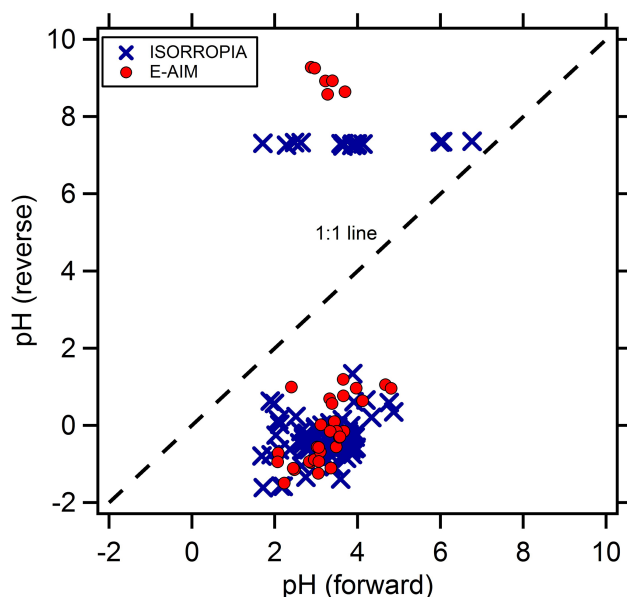
Figure 1. Comparison of pH predicted using the reverse and forward modes of ISORROPIA and E-AIM.

for the present analysis only if the above criteria were met, and both the NH$_3$ and HNO$_3$ measurements were operational for a given sampling interval. These constraints explain the differences in sample numbers between the forward and reverse simulations and between E-AIM and ISORROPIA (Table 2). ISORROPIA-II model runs were performed in "metastable" mode where the aerosol is only in the aqueous phase and can be supersaturated (http://isorropia.eas.gatech. edu/). ISORROPIA treats the Na$^+$–NH$_4^+$–K$^+$–Ca^{2+}–Mg^{2+}–Cl$^-$–NO$_3^-$–SO$_4^{2-}$ system. For conditions of excess cations, ISORROPIA-II assumes that bicarbonate (HCO$_3^-$) and carbonate (CO$_3^{2-}$) account for the deficit, and a pH limit of 7 is imposed. Model version AIM-IV was used for RH conditions greater than 60 % ($n = 348$, Table 2), and model version AIM-II was used for RH conditions between 40 and 60 % ($n = 112$, Table 2) (http://www.aim.env.uea.ac.uk/aim/aim. php). AIM-IV treats the Na$^+$–NH$_4^+$–Cl$^-$–NO$_3^-$–SO$_4^{2-}$ system, while AIM-II treats NH$_4^+$–NO$_3^-$–SO$_4^{2-}$. For AIM, measured cations not treated by the model were accounted for as equivalent sodium (Na*) in AIM-IV and equivalent ammonium (NH$_4^*$) in AIM-II. Cl$^-$ was accounted for as equivalent sulfate (SO$_4$*) in AIM-II. Ion balance is required for all simulations in E-AIM: any cation deficit was balanced using H$^+$, while any anion deficit was balanced using OH$^-$ since these are also required model inputs. E-AIM assumes that OH$^-$ balances any excess cations, rather than carbonate, and thus has regions of higher predicted aerosol pH compared with ISORROPIA.

E-AIM model runs were performed in solid + liquid mode where salts precipitate once the aqueous solution becomes saturated. Overall, strong similarities between E-AIM and

ISORROPIA suggest that the choice of metastable vs. stable (solid + liquid) mode did not appreciably affect the predicted aerosol pH levels. Given the importance of aerosol liquid water, data below 40 % RH were excluded from the analysis. During the MILAGRO study, this was approximately 50 % of the total measurement period. Further, points above 40 % RH with modeled aerosol liquid water content of 0 were excluded from the analysis since a pH cannot be derived for these samples. This was the cause of differences in sample numbers between the E-AIM and ISORROPIA simulations (Table 2).

3 Results and discussion

3.1 Thermodynamic equilibrium models

Thermodynamic equilibrium models are frequently used to estimate aerosol acidity. Prior studies have observed and discussed large differences in aerosol acidity predicted by different models (Ansari and Pandis, 1999; Yao et al., 2006); we do not revisit this analysis but instead seek to understand some of the limitations and uncertainties of using thermodynamic equilibrium models to predict aerosol pH. Figure 1 shows that a large source of uncertainty is tied to the availability of gas-phase data and whether the model is run in the forward (gas + aerosol inputs) or reverse (aerosol inputs only) mode. Note that the number of forward-mode predictions was less than the reverse-mode predictions due to availability of coincident aerosol- and gas-phase measurements. For ISORROPIA and E-AIM, the median differences between the models run in forward and reverse modes were 3.5 and 3.1 pH units, respectively. This finding is consistent with a modeling study of aerosol pH in Hong Kong as well (Yao et al., 2006). Other parameters, such as aerosol liquid water, have much closer agreement between the forward and reverse modes (not shown), given that it is largely driven by total aerosol mass and, thus, is much less sensitive to gas-phase species.

The large differences in the forward- and reverse-mode predictions of aerosol pH seen in Fig. 1 come about for several reasons. Upon specification of the aerosol species and surrounding RH and T, thermodynamic models first determine the aerosol pH and liquid water content (assuming that a liquid phase can exist), followed by computing the concentration of gas-phase semi-volatile compounds in equilibrium with the aerosol (e.g., NH$_3$, HNO$_3$, and HCl). The aerosol pH is largely driven by electroneutrality in the aqueous phase, as any imbalance between charges from cations and anions needs to be balanced by H$^+$ and OH$^-$:

$$\left[H^+\right] + \sum_{n+}\left[X^+\right] = \left[OH^-\right] + \sum_{n-}\left[Y^-\right],$$

$$\text{or}\left[H^+\right] + I_b - \left[OH^-\right] = 0, \tag{7}$$

where $I_b = \sum_{n+}\left[X^+\right] - \sum_{n-}\left[Y^-\right]$ is the ion balance parameter; n^+ and n^- are the number of positively and nega-
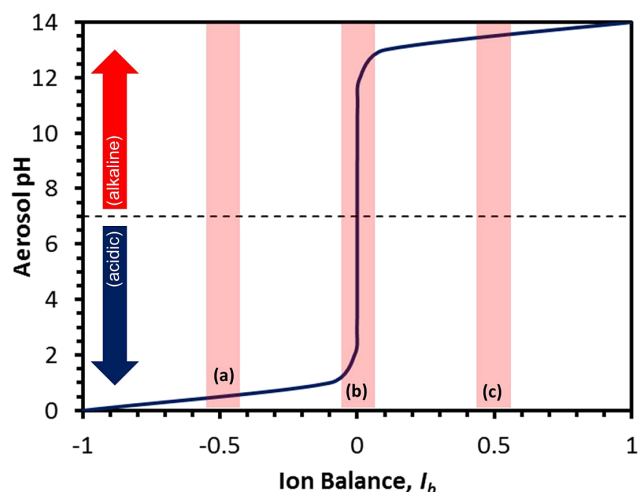
Figure 2. Aerosol pH as a function of the parameter I_b (see Eq. 7 for explanation). The data used here are hypothetical: values of I_b ranging from -1 to 1 at a constant aerosol loading were input under conditions of constant T and RH to demonstrate the extreme sensitivity of aerosol pH at I_b values near 0.0 (region b).
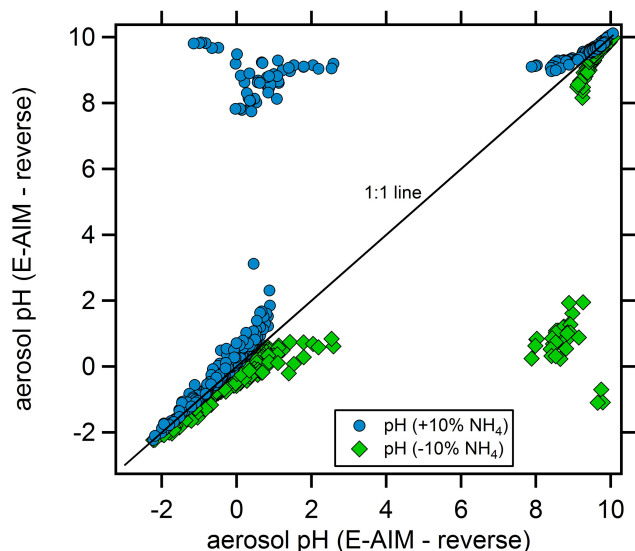
Figure 3. Sensitivity of aerosol pH predicted with E-AIM (reverse mode) to small changes in the input aerosol NH_4^+ concentration.

tively charged ionic species, respectively; and $[X^+]$ is the concentration of a species in the aqueous phase, in gram equivalents (geq). In the case where the aerosol is acidic (i.e., pH < 7 or $I_b < -\sqrt[2]{K_w}$, with $K_w = [OH^-][H^+]$), $[OH^-]$ contributes negligibly to I_b, and $[H^+] \cong -I_b$. Similarly, when the aerosol is alkaline (i.e., pH > 7 or $I_b > \sqrt[2]{K_w}$), $[H^+]$ contributes negligibly to I_b, $[OH^-] \cong I_b$, and $[H^+] = K_w / [OH^-]$.

Given the above, one can construct a diagram that relates aerosol pH to I_b; this is shown in Fig. 2. It is noteworthy that

pH changes considerably over a narrow range of I_b, when the value of I_b is close to 0. For acidic and very alkaline aerosol, uncertainty in I_b – shown as the (a) and (c) regions of Fig. 2 – may introduce a 0.5–1.0 pH unit bias in predicted pH. In region (b), however, a small uncertainty in I_b leads to shifts in pH that span effectively 10 pH units (or more). This uncertainty may come from either uncertainty in the measurements, themselves, or from approximations such as the exclusion of minor species (e.g., crustal elements) from the analysis. The data used in Fig. 2 are hypothetical: values of I_b ranging from -1 to 1 at a constant aerosol loading were input under conditions of constant T and RH to generate the predicted pH. However, Fig. 3 shows that for the MILAGRO data set, the predicted aerosol pH (reverse mode) is extremely sensitive to minor uncertainties in the measurement inputs and, thus, to uncertainties in I_b. Figure 3 shows the sensitivity in predicted aerosol pH under the reverse-mode calculation to $\pm 10\%$ changes in the aerosol NH_4^+ concentration. The aerosol pH differed by more than 1.0 pH unit for 18 % of the data when NH_4^+ increased by 10 %. Likewise, aerosol pH differed by more than 1.0 pH unit for 12 % of the data when NH_4^+ decreased by 10 %. Similar sensitivities were also observed for $\pm 10\%$ changes in aerosol NO_3^- and SO_4^{2-} inputs. Using gas + aerosol inputs strongly constrains the effects of measurement errors and therefore is thought to give a more accurate representation of aerosol partitioning and composition (Fountoukis et al., 2009; Guo et al., 2014). Our results support this thought and indicate that reverse-mode calculations of aerosol H^+ and pH should likely be avoided for the interpretation of experimental data. The exception to this recommendation would be a system that contains very low concentrations of semi-volatiles. Without accompanying gas-phase data to constrain the thermodynamic models, an alternate approach that may yield a more accurate representation of aerosol pH is the use of aerosol concentrations as input in forward-mode calculations. In the southeastern US, Guo et al. (2014) report that this approach led to biases in aerosol pH of $\sim$ 1 pH unit, which is considerably lower than the bias observed in Fig. 1 if we assume that the forward-mode predictions are accurate (see more discussion on this point below).

3.2 Phase partitioning

Figure 4 shows aerosol pH predicted by ammonia phase partitioning vs. aerosol pH predicted by E-AIM and ISOR-ROPIA run in the forward and reverse modes. To predict aerosol pH from the NH_3 / NH_4^+ phase equilibrium (Eq. 6), aerosol liquid water was taken from the forward model output of ISORROPIA. The temperature-dependent K_H and K_b are from Chameides (1984), while the temperature-dependent K_w is from Stumm and Morgan (1996). We have used liquid concentrations, not activities in the application of Eq. (6) (i.e., activity coefficients for H^+ and NH_4^+ are assumed to be unity), following the approach of Keene
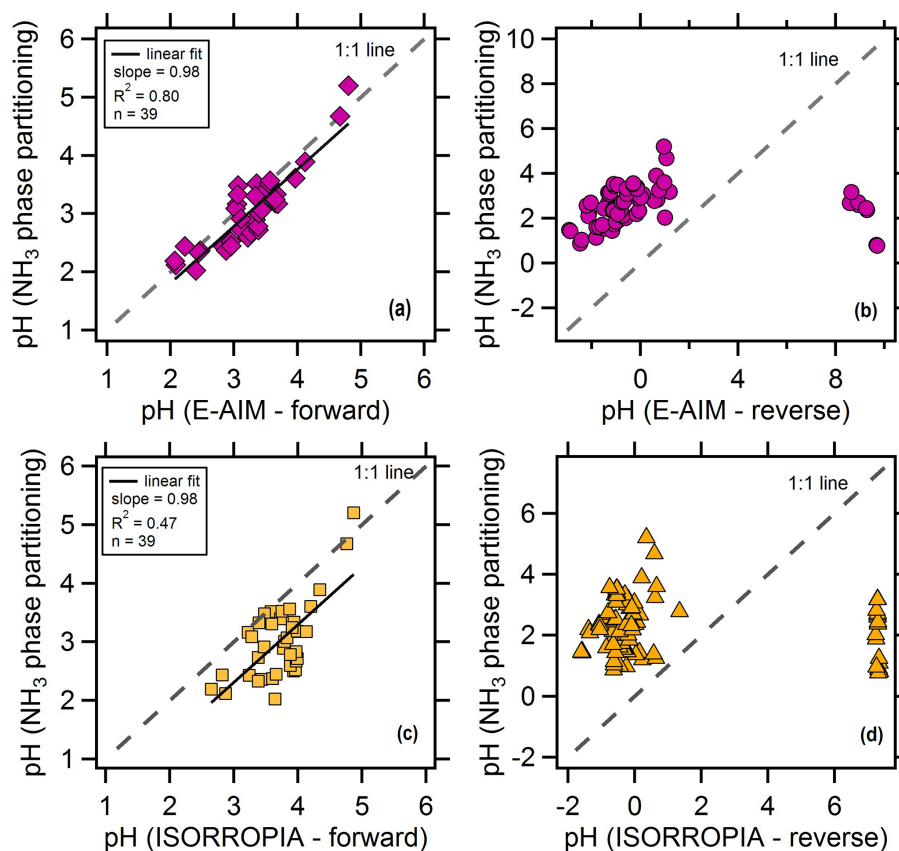
**Figure 4.** Aerosol pH predicted by the phase partitioning of ammonia compared to pH predicted by **(a)** E-AIM in the forward mode, **(b)** E-AIM in the reverse mode, **(c)** ISORROPIA in the forward mode, and **(d)** ISORROPIA in the reverse mode.

et al. (2004). The implications of these assumptions are discussed below. The best agreement between the phase-partitioning approach and the models was found for both forward model applications (Fig. 4a and c). A slope of 0.98 and high R^2 value (0.80) indicate excellent agreement between E-AIM and the phase-partitioning approach (Fig. 4a). The median difference between these methods was only 0.4 pH unit. Likewise, good agreement was observed between ISORROPIA-II in the forward mode and the phase-partitioning pH (Fig. 4c, slope = 0.98 and $R^2 = 0.47$).

Differences between the NH_3 / NH_4^+ phase-partitioning predictions and either thermodynamic model are possibly due to differences in equilibrium constants and/or differences in the activity coefficients, although the former is more likely. That is evident from the strong agreement seen in Fig. 4a; since E-AIM employs activity coefficient calculations for all species, our calculation using concentrations instead of activities does not appear to systematically bias the phase-partitioning pH predictions. A detailed characterization of uncertainties and sensitivities of the various methods to differences in equilibrium constants and activity coefficients is beyond the scope of this study but should be explored in the future.

The above results were contrasted by very poor agreement between the reverse models and phase-partitioning predictions of aerosol pH (Fig. 4b and d). The median difference between aerosol pH predicted by NH_3 phase partitioning and E-AIM run in the reverse mode was 3.5 pH units ($n = 72$). Similarly, the median difference between aerosol pH predicted by NH_3 phase partitioning and ISORROPIA-II run in reverse mode was 3.1 pH units ($n = 72$). These large differences are consistent with the large differences observed between the forward and reverse predictions of pH (Fig. 1). These results are also consistent with large discrepancies (on the order of 1–4 pH units) in aerosol pH between E-AIM run in the reverse mode and the phase-partitioning approach for a study in Hong Kong (Yao et al., 2006). As discussed above, gas + aerosol inputs constrain the effects of measurement uncertainty on thermodynamic models, and thus the large differences observed in Fig. 4b and d provide further support that the reverse model applications are challenged to accurately predict aerosol pH. For the MILAGRO data set, approximately half of all reverse model runs predicted pH values less than 0 (44 % for E-AIM, 51 % for ISORROPIA). This is inconsistent with the observed aerosol ammonium fraction ($NH_4^+ / (NH_3 + NH_4^+)$), which was only
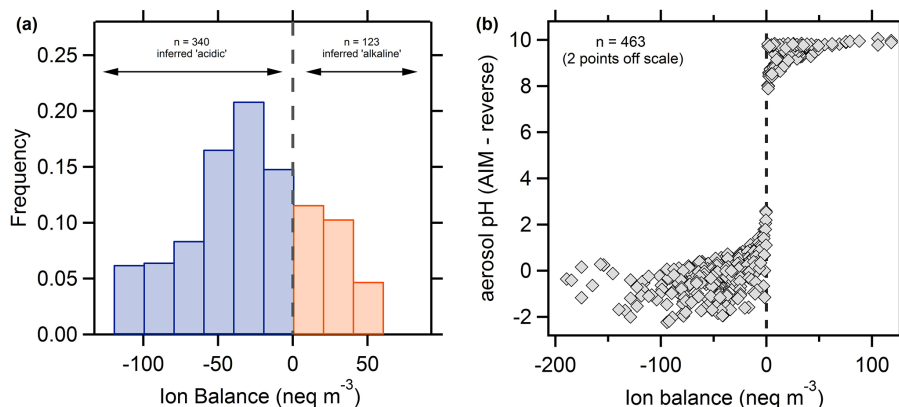
Figure 5. (a) Frequency distribution of the aerosol ion balance during MILAGRO, and **(b)** aerosol pH predicted by E-AIM in the reverse mode vs. the ion balance. The dashed lines at 0 serve as a visual reference for neutral particles.

0.2, on average, over the study period. Under conditions typical of the MILAGRO study (293 K, 10 µg m^{-3} aerosol liquid water, total NH$_3$ of 10–30 µg m^{-3}), if the aerosol pH is less than 0, thermodynamic calculations predict that essentially all of the NH$_3$ will partition to the particle phase at equilibrium. The fact that gas-phase NH$_3$ was abundant (Table 1) suggests either that (1) the system is not at equilibrium or that (2) aerosol pH > 0. Fountoukis et al. (2009) found that the equilibration timescales for NH$_3$ / NH$_4^+$ (approximately 10 min) were on par with the measurement integration timescales during MILAGRO, strongly suggesting that the assumption of equilibrium is valid. This further supports the conclusion above that the reverse-mode models vastly overstate the acidity (underestimate pH) of the Mexico City aerosol.

These results suggest that the two best proxy methods for estimating aerosol pH are (1) thermodynamic equilibrium models run using gas + aerosol inputs, and (2) the phase partitioning of ammonia. Under certain conditions, the phase partitioning of HNO$_3$ / NO$_3^-$ gives similar results to that of ammonia (Young et al., 2013), so this is another feasible approach. It should be noted that Young et al. (2013) caution against the use of HCl / Cl$^-$ partitioning to estimate pH on the basis of large (order of magnitude) uncertainty in the Henry's law constant for HCl. It should also be noted that Keene et al. (2004) observed relatively poor agreement between pH predicted by ammonia and nitric acid phase partitioning. This may be due to the explicit treatment of activity coefficients (as was done by Young et al., 2013), or to differences in other factors, such as relative ammonia levels, since this can introduce major differences in thermodynamic model predictions (Ansari and Pandis, 1999). Other limitations of the phase-partitioning approach should be considered, depending on the environment. This includes long equilibration timescales for coarse particles and the presence of insoluble or partially soluble salts (Jacobson, 1999; Fridlind and Jacobson, 2000; Meng and Seinfeld, 1996).

3.3 Ion balance vs. aerosol pH

Figure 5a shows a probability distribution for the ion balance during MILAGRO. All of the measured inorganic species (Sect. 2.5) were included in the calculation according to Eq. (2), but dissociated organic acids were not included since they were not measured. Approximately 75 % of the paired cation–anion measurements had a cation deficit and would thus be inferred as acidic according to the ion balance. Figure 5b shows the aerosol pH predicted by E-AIM (reverse mode) vs. the inorganic ion balance. The data follow the traditional titration curve shape, with those points having a negative ion balance (anions > cations) all having predicted pH below 3.0 and points having a positive ion balance (cations > anions) all having predicted pH above 7.8.

The ion balance proxy method assumes that conditions of high aerosol H$^+$ loading (in nmol m^{-3}) correspond to an aerosol distribution with a low (acidic) pH (e.g., Feng et al., 2012; Zhang et al., 2012a). Figure 6 shows the relationship between predicted aerosol pH and the H$^+$ concentration inferred from the ion balance. An anion deficit in the ion balance is assumed to be due to OH$^-$ (Eq. 2) – implying extremely low H$^+$ levels – so only data with a negative ion balance were included in this analysis ($n = 340$). Figure 6 shows no correlation at all between the H$^+$ loading and the predicted aerosol pH using either the forward (Fig. 6a) or reverse models (Fig. 6b). Note the differences in pH predicted by the forward and reverse models, as observed in Fig. 1. Numerous points in the lowest H$^+$ quartile have pH levels below the median pH of the upper H$^+$ quartile (Fig. 6b). Similarly, for a given H$^+$ loading, a wide pH range of $\sim$ 2–3 pH units is typically predicted. This wide pH range is observed across all H$^+$ loadings, even at the high and low ends, because aerosol liquid water content and the H$^+$ activity coefficient can differ dramatically for a given H$^+$ level. The ion balance method is insensitive to either of these factors that are critical in determining aerosol pH (Eq. 1). Pathak et al. (2009) found a simi-
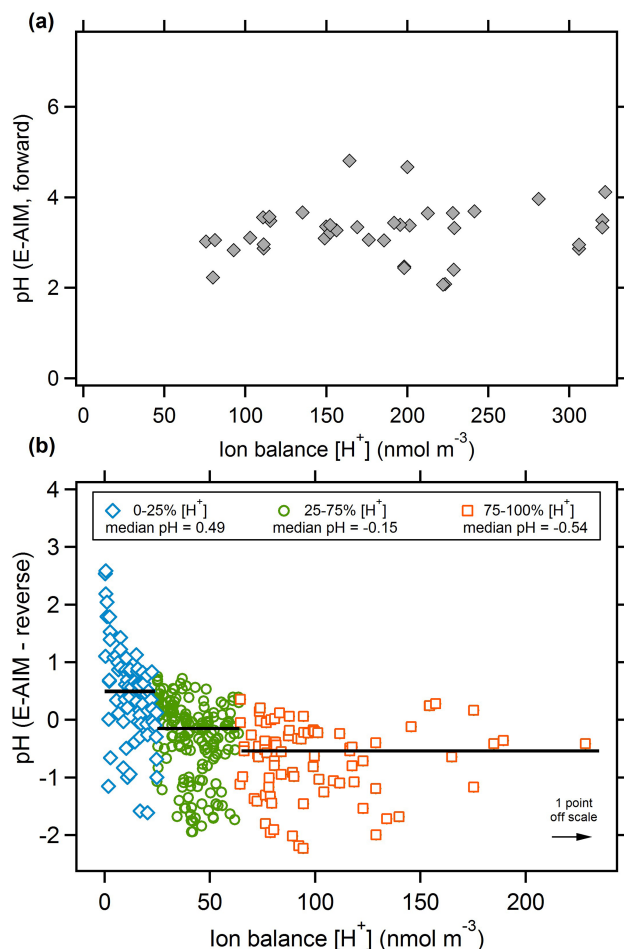
Figure 6. (a) Aerosol pH predicted by E-AIM in the forward mode vs. the H^+ concentration derived from the ion balance, and **(b)** aerosol pH predicted by E-AIM in the reverse mode vs. the H^+ concentration derived from the ion balance. Only points with a cation charge deficit ($\Sigma(\text{anions}) > \Sigma(\text{cations})$) are included in the analysis in **(b)**. The horizontal black bars in **(b)** represent the medians corresponding to the values in the legend.

lar disconnect between H^+ inferred from the ion balance and predicted aerosol pH for measurements in four cities across China.

A further problem with the ion balance is that it is unable to distinguish between free and undissociated H^+ (e.g., protons associated with bisulfate (HSO_4^-)); Keene et al., 2004). This limitation becomes very important when the solution pH approaches the pK_a of any major ion that is associated with acidity, including HNO_3, HCl, and NH_3. The pK_a of HSO_4^- is 1.99 (Stumm and Morgan, 1996), and at pH levels below 3 the bisulfate–sulfate equilibrium begins to shift appreciably towards the protonated form, implying that the ion balance overestimates H^+. This is illustrated in Fig. 7a and b, which shows the H^+ levels inferred from the ion balance compared to the H^+ loadings predicted by E-AIM and ISORROPIA (both run in reverse mode), respectively. Although the ther-

modynamic models use electroneutrality to derive H^+, they account for partial dissociation, which explains why the ion balance gives H^+ levels that are $\sim$ 45–65 % higher than the models. The discrepancy in pH predicted by the forward- and reverse-mode thermodynamic calculations (Figs. 1 and 6) also implies large differences in the predicted aerosol H^+ loadings. Figure 7c and d shows H^+ levels inferred from the ion balance compared to H^+ levels predicted by E-AIM and ISORROPIA, both run in forward mode. The forward-mode thermodynamic calculations predict H^+ levels that are orders of magnitude lower than either the ion balance or reverse-mode calculations, consistent with the large differences in predicted pH shown in Fig. 1. This is also consistent with large discrepancies in H^+ levels in Pittsburgh, PA, predicted by forward (Takahama et al., 2006) and reverse (Zhang et al., 2007) thermodynamic equilibrium model simulations. Although the measurement periods for these studies in Pittsburgh did not overlap, the similar NH_4^+ and SO_4^{2-} concentrations suggest that the large differences in aerosol H^+ were likely due to differences in the forward and reverse model simulations, not in the actual pH levels of the aerosol.

Finally, another major limitation in estimating the aerosol H^+ loading from the ion balance is high uncertainty in H^+ that comes about from the propagation of measurement error. Figure 8a shows the relative ion balance uncertainty (%) vs. the ion balance loading (nmol m^{-3}). Note that the points with a negative ion balance (orange trace in Fig. 8a) are inferred as the H^+ loading, and so this trace also represents the uncertainty in H^+ from the ion balance. The ion balance uncertainty was calculated using a standard propagation-of-error technique (Harris, 1999):

$$u_{IB} = (u_{Na^+}^2 + u_{NH_4^+}^2 + u_{Mg^{2+}}^2 + u_{Ca^{2+}}^2 + u_{K^+}^2 + u_{Cl^-}^2 + u_{NO_3^-}^2 + u_{SO_4^{2-}}^2)^{\frac{1}{2}}, \qquad (8)$$

where u_{IB} is the absolute uncertainty in the ion balance (in neq m^{-3}), and the terms on the right-hand side represent the absolute uncertainties in each inorganic species in neq m^{-3} (Na^+, NH_4^+, Mg^{2+}, Ca^{2+}, K^+, Cl^-, NO_3^-, and SO_4^{2-}), calculated assuming 10 % relative uncertainty for each species. Figure 8a shows that the relative ion balance (and $[H^+]$) uncertainty ($u_{IB}/[\text{ion balance}]$) grows with decreasing ion balance or $[H^+]$, as one would expect. A frequency distribution of the ion balance uncertainty from the MILAGRO study shows that approximately 40 % of the ion balance and $[H^+]$ calculations had an associated uncertainty higher than 50 %, and more than 20 % of the ion balance and $[H^+]$ calculations had an associated uncertainty higher than 100 % (Fig. 8b).

These results demonstrate numerous problems with the ion balance and strongly suggest that it is inadequate to represent the pH of atmospheric particles. The ion balance may provide a qualitative indication of acidic conditions when anions far exceed cations, but the variable effects of liquid water, the buffering action of HSO_4^- / SO_4^{2-}, and the effect of species
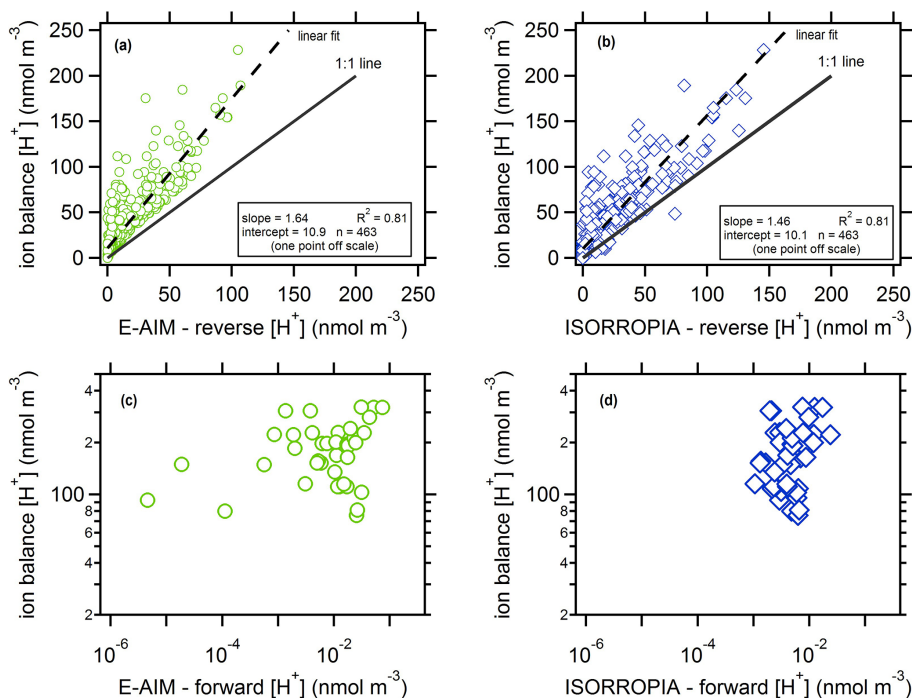
Figure 7. H$^+$ levels inferred from the ion balance compared to H$^+$ levels predicted by **(a)** E-AIM in the reverse mode, **(b)** ISORROPIA in the reverse mode, **(c)** E-AIM in the forward mode, and **(d)** ISORROPIA in the forward mode. Note the different log scales for the x and y axes in **(c)** and **(d)**.
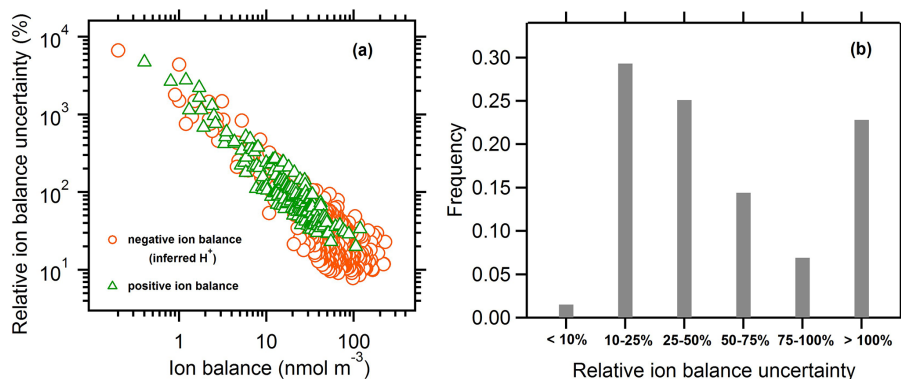
Figure 8. (a) Relative ion balance uncertainty (%) as a function of the ion balance level. Note that the orange trace represents [H$^+$], and so this trace also represents the uncertainty in [H$^+$] from the ion balance. **(b)** Frequency distribution in the relative ion balance uncertainty.

activity coefficients in concentrated particles preclude its use for any quantitative means. Even when all ionic components – including the dissociated ions of organic acids – are accounted for and measured with good precision, the ion balance is unlikely to qualitatively distinguish alkaline particles from mildly acidic particles due to the propagation of uncertainties in the aerosol composition measurements. This recommendation against the use of the ion balance as a proxy for aerosol pH is supported by prior work (Keene and Savoie, 1998; Winkler, 1986; Guo et al., 2014). The H$^+$ concentration derived from the ion balance is often just a surrogate

for sulfate, especially in environments where sulfate is the dominant inorganic species (Pathak et al., 2009; Zhang et al., 2007). It is possible – likely even – to simultaneously have particles with a low concentration of H$^+$ (in nmol m^{-3}) that are highly acidic (low pH). Studies that infer the effects of particle acidity on atmospheric chemical processes using the inorganic ion balance are likely flawed. For example, correlations between SOA and aerosol H$^+$ concentrations from the ion balance have been interpreted as evidence of acid-catalyzed SOA formation (Feng et al., 2012; Budisulistiorini et al., 2013; Pathak et al., 2011; Nguyen et al., 2014; Zhang et
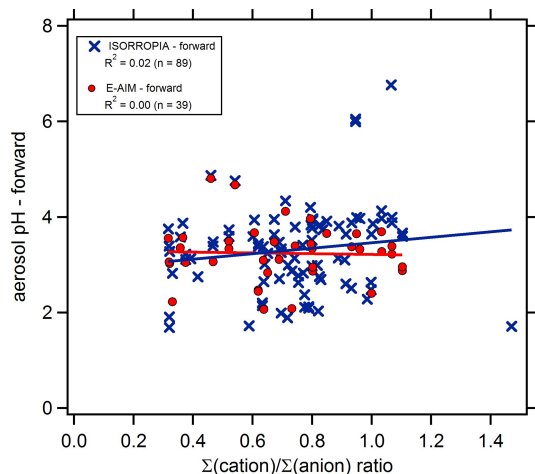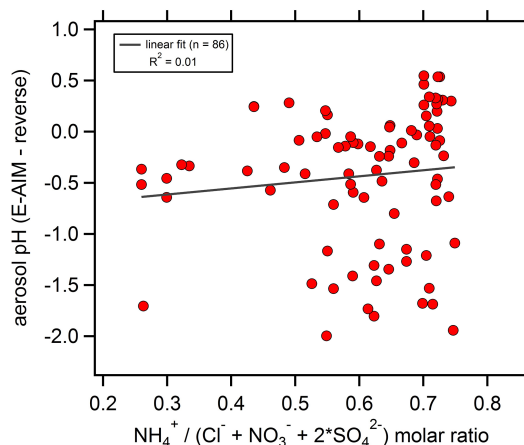
Figure 9. Aerosol pH predicted by the forward-mode equilibrium models compared to the Σ(cations)/Σ(anions) charge ratio.

Figure 10. Predicted aerosol pH vs. the $NH_4^+ / (Cl^- + NO_3^- + 2*SO_4^{2-})$ molar ratio, using only data where the ratio is less than 0.75 (region inferred as highly acidic) and where $\Sigma(NH_4^+ + Cl^- + NO_3^- + SO_4^{2-})$ accounts for greater than 95 % of measured inorganic aerosol mass (i.e., with low crustal concentrations).

al., 2012a). These studies may have misinterpreted their data, since sulfate may actually be a limiting factor in isoprene and monoterpene SOA formation (Xu et al., 2015). H^+ derived from the ion balance is a surrogate for sulfate, and many factors lead to correlations between sulfate and SOA in regional pollution (Sun et al., 2011; Zhang et al., 2012b).

3.4 Molar ratio vs. pH

Similar to applications of the ion balance, the molar ratio is frequently used as a proxy for aerosol pH. Molar ratios that yield a charge balance (i.e., equivalence ratios of unity or greater) are assumed for fully neutralized aerosol, while decreasing cation/anion ratios are assumed to represent decreasing aerosol pH (He et al., 2012; Kerminen et al., 2001; Huang et al., 2013). The data and assumptions that underlie the molar ratio method are the same as those used to calculate the ion balance. Thus, many of the same limitations apply to the molar ratio method. The exclusion of minor ionic species, including crustal elements and dissociated organic acids, can significantly bias the results (Cao et al., 2013; Jacobson, 1999; Trebs et al., 2005; Ziemba et al., 2007; Moya et al., 2002). The propagation of analytical uncertainty can also create problems with the signal-to-noise ratio for many samples that will challenge the interpretations of the molar ratio. Finally, the molar ratio does not account for the effects of aerosol water or species activities on particle acidity. Given the similar assumptions and limitations, it should be unsurprising that [H^+] from the ion balance was highly correlated with the cation/anion molar ratio ($R^2 = 0.66$, not shown) for the MILAGRO data set. Similar to the ion balance results, no correlation was observed between the molar ratio and forward-mode predictions of aerosol pH (Fig. 9). Zhang et al. (2007) and Behera et al. (2014) demonstrated similar problems translating the molar ratio into aerosol pH for studies in Pittsburgh and Singapore, respectively. Even

under the limiting case when (1) crustal elements were low (where NH_4^+, Cl^-, NO_3^-, and SO_4^{2-} together accounted for greater than 95 % of inorganic aerosol ion mass) and (2) the aerosol regime was inferred to be highly acidic (samples with $NH_4^+ / (Cl^- + NO_3^- + 2*SO_4^{2-})$ molar ratios less than 0.75), there was no correlation between the molar ratio and predicted pH (Fig. 10).

These results indicate that the molar ratio is not a suitable proxy to infer the acidity of atmospheric particles. This applies to all variations of the molar ratio (Eqs. 3, 4, or 5). When the majority of inorganic species (> 95 %) are accounted for, the molar ratio is able to distinguish alkaline particles from acidic particles with good reliability; however, it is unable to provide any measure – even qualitative – of the degree of aerosol acidity. The lack of relationship between the molar ratio and predicted aerosol pH strongly suggests problems with studies that have used the molar ratio as a proxy for pH. For example, studies that have attempted to characterize the occurrence of acid-catalyzed SOA formation in the atmosphere may have incorrectly interpreted the aerosol acidity using a molar ratio approach (e.g., Tanner et al., 2009; Peltier et al., 2007; Zhang et al., 2007; Froyd et al., 2010).

4 Conclusions

We have carried out an analysis of proxy methods used to estimate the pH of atmospheric particles. The ion balance method, which is used to infer the aerosol H^+ loading, showed no correlation with aerosol pH predicted by multiple independent metrics. This indicates that conditions of increasing H^+ loading do not necessarily correspond to decreasing (i.e., more acidic) aerosol pH. Likewise, the cation/anion molar ratio (and related metrics) showed no

relationship with different predictions of aerosol pH. When species accounting for greater than 95 % of inorganic aerosol mass were included in the analysis, the molar ratio appears to reliably distinguish acidic from alkaline particles; however, the molar ratio should not be treated as a surrogate for aerosol pH. The molar ratio actually showed a strong relationship with the ion balance. A major reason for the inability of these methods to represent aerosol pH is that both neglect the effects of aerosol water and partial dissolution of ions and acids on pH, in accordance with previously published studies (Keene and Savoie, 1998; Winkler, 1986). Further, the ion balance and molar ratio can also be severely limited by signal-to-noise ratio due to analytical uncertainties. These results strongly discourage the use of the ion balance or molar ratio for pH or H^+ inference.

These results also suggest that thermodynamic equilibrium models require both gas + aerosol inputs for accurate predictions of H^+ and pH. Two independent models – E-AIM and ISORROPIA – performed similarly and predict much lower pH (more acidic particles) in the reverse modes using aerosol inputs only. The aerosol pH levels predicted by both reverse models do not agree with either the pH predictions using gas + aerosol inputs or the phase partitioning of ammonia. The models in reverse mode predict highly acidic particles for extended periods of time (i.e., pH < 0), despite high concentrations of gas-phase ammonia and relatively short equilibration timescales. Further, the models in reverse mode are highly sensitive to uncertainty in the measurement inputs: small deviations in major aerosol species on the order of common aerosol measurement uncertainties can induce changes in predicted pH that exceed 10 pH units. This recommendation is consistent with other studies that show much better model performance when aerosol + gas inputs are used (Fountoukis et al., 2009; Guo et al., 2014).

Thermodynamic equilibrium models in forward mode had very good agreement with pH predicted by the phase partitioning of ammonia. These methods are largely, but not completely, independent, as the aerosol liquid water required for the phase-partitioning calculation is obtained from the same thermodynamic models. In addition, the use of activity coefficients from thermodynamic models as inputs in the phase-partitioning calculations would further couple the two methods. This has been avoided in the present analysis by using concentrations instead of activities. Thermodynamic equilibrium models are generally quite skilled in predicting aerosol liquid water (Khlystov et al., 2005), so this likely introduces minimal uncertainty to the present analysis. In regions where organics are high, their contribution to aerosol liquid water (and hence pH) should be investigated (Guo et al., 2014). The fact that these largely independent methods agreed so closely provides the basis for the recommendation of their use to estimate the pH of atmospheric particles. As with the application of thermodynamic equilibrium models, the phase-partitioning approach makes the implicit assumption that the gas/particle system is at equilibrium. This

appears to be a good assumption for the Mexico City data set (Fountoukis et al., 2009), but it can be a poor assumption when coarse particles are abundant, such as in the marine environment (Fridlind and Jacobson, 2000). The phase-partitioning approach is also likely limited in ammonia-poor environments where all or most of the ammonia resides in the aerosol phase. In such environments, the phase partitioning of nitric acid may be a good alternative if both nitric acid and aerosol nitrate concentrations are high enough (Young et al., 2013; Meskhidze et al., 2003). Uncertainty in the Henry's law constant of other compounds, especially HCl, may limit the application of the phase-partitioning approach beyond NH_3 / NH_4^+ and HNO_3 / NO_3^- (Young et al., 2013).

Our recommendation for the use of the phase-partitioning approach and forward equilibrium model calculations to best predict aerosol pH contradicts the recommendations in a similar study (Yao et al., 2006). Both our study (from Mexico City) and the Yao et al. (2006) study (Hong Kong) agree that E-AIM run in the reverse mode yields predicted aerosol pH levels significantly lower than the phase partitioning or forward model predictions. We differ in our interpretation of the results: Yao et al. (2006) conclude that the phase-partitioning approach and forward model calculations erroneously assume that the gas–aerosol system has reached equilibrium, even though their analysis is based upon 12 and 24 h $PM_{2.5}$ measurements. This sampling time should far exceed the equilibrium time for submicron particles, which is on the order of seconds to minutes (Meng and Seinfeld, 1996). In addition, our comparisons in Fig. 4a and c only include the subset of data where RH exceeds 60 %, a region in which the thermodynamic predictions – and assumption of equilibrium – become more accurate (Moya et al., 2002). Fountoukis et al. (2009) examined the equilibrium assumption for $PM_{2.5}$ during MILAGRO and found it to be valid. Thus, we believe that the forward thermodynamic models and phase-partitioning approach are far more accurate in their predictions of pH than the reverse models run in closed mode without the additional constraint of gas-phase data.

These recommendations should be evaluated in other environments with different chemical characteristics and meteorology than was observed during MILAGRO. In particular, the recommendations should be evaluated in ammonia-poor environments, since thermodynamic equilibrium models often diverge in their predictions under such conditions (Ansari and Pandis, 1999). Despite their uncertainties, thermodynamic models and phase partitioning provide the best methods to estimate the pH of fine atmospheric particles. Other widely used metrics – ion balance and ion ratios – are misleading and should be avoided beyond the establishment of general alkalinity or acidity. Hence, conclusions that are sensitive to aerosol pH but that are based upon the ion balance or molar ratio may need revision.

Edited by: A. Kiendler-Scharr

References

Ahrens, L., Harner, T., Shoeib, M., Lane, D. A., and Murphy, J. G.: Improved Characterization of Gas-Particle Partitioning for Per- and Polyfluoroalkyl Substances in the Atmosphere Using Annular Diffusion Denuder Samplers, Environ. Sci. Technol., 46, 7199–7206, doi:10.1021/Es300898s, 2012.

Ansari, A. S. and Pandis, S. N.: An analysis of four models predicting the partitioning of semivolatile inorganic aerosol components, Aerosol. Sci. Tech., 31, 129–153, doi:10.1080/027868299304200, 1999.

Behera, S., Cheng, J., and Balasubramanian, R.: In situ acidity and pH of size-fractionated aerosols during a recent smoke-haze episode in Southeast Asia, Environ. Geochem. Hlth., 1–17, doi:10.1007/s10653-014-9660-1, 2014.

Brown, S. S., Thornton, J. A., Keene, W. C., Pszenny, A. A. P., Sive, B. C., Dube, W. P., Wagner, N. L., Young, C. J., Riedel, T. P., Roberts, J. M., VandenBoer, T. C., Bahreini, R., Ozturk, F., Middlebrook, A. M., Kim, S., Hubler, G., and Wolfe, D. E.: Nitrogen, Aerosol Composition, and Halogens on a Tall Tower (NACHTT): Overview of a wintertime air chemistry field study in the front range urban corridor of Colorado, J. Geophys. Res.-Atmos., 118, 8067–8085, doi:10.1002/Jgrd.50537, 2013.

Budisulistiorini, S. H., Canagaratna, M. R., Croteau, P. L., Marth, W. J., Baumann, K., Edgerton, E. S., Shaw, S. L., Knipping, E. M., Worsnop, D. R., Jayne, J. T., Gold, A., and Surratt, J. D.: Real-Time Continuous Characterization of Secondary Organic Aerosol Derived from Isoprene Epoxydiols in Downtown Atlanta, Georgia, Using the Aerodyne Aerosol Chemical Speciation Monitor, Environ. Sci. Technol., 47, 5686–5694, doi:10.1021/Es400023n, 2013.

Cao, J. J., Tie, X. X., Dabberdt, W. F., Jie, T., Zhao, Z. Z., An, Z. S., Shen, Z. X., and Feng, Y. C.: On the potential high acid deposition in northeastern China, J. Geophys. Res.-Atmos., 118, 4834–4846, doi:10.1002/Jgrd.50381, 2013.

Chameides, W. L.: The photochemistry of a remote marine stratiform cloud, J. Geophys. Res.-Atmos., 89, 4739–4755, 10.1029/JD089iD03p04739, 1984.

Clegg, S. L., Brimblecombe, P., and Wexler, A. S.: Thermodynamic model of the system H^+-NH_4^+-SO_4^{2-}-NO_3^--H_2O at tropospheric temperatures, J. Phys. Chem. A, 102, 2137–2154, doi:10.1021/Jp973042r, 1998.

Clegg, S. L., Seinfeld, J. H., and Edney, E. O.: Thermodynamic modelling of aqueous aerosols containing electrolytes and dissolved organic compounds. II. An extended Zdanovskii-Stokes-Robinson approach, J. Aerosol Sci., 34, 667–690, doi:10.1016/s0021-8502(03)00019-3, 2003.

Day, D. A., Wooldridge, P. J., Dillon, M. B., Thornton, J. A., and Cohen, R. C.: A thermal dissociation laser-induced fluorescence instrument for in situ detection of NO_2, peroxy nitrates, alkyl nitrates, and HNO_3, J. Geophys. Res.-Atmos., 107, 4046, doi:10.1029/2001jd000779, 2002.

Dockery, D. W., Cunningham, J., Damokosh, A. I., Neas, L. M., Spengler, J. D., Koutrakis, P., Ware, J. H., Raizenne, M., and Speizer, F. E.: Health effects of acid aerosols on North American children: Respiratory symptoms, Environ. Health Persp., 104, 500–505, doi:10.2307/3432990, 1996.

Farmer, D. K., Perring, A. E., Wooldridge, P. J., Blake, D. R., Baker, A., Meinardi, S., Huey, L. G., Tanner, D., Vargas, O., and Cohen, R. C.: Impact of organic nitrates on urban ozone production, Atmos. Chem. Phys., 11, 4085–4094, doi:10.5194/acp-11-4085-2011, 2011.

Feng, J. L., Guo, Z. G., Zhang, T. R., Yao, X. H., Chan, C. K., and Fang, M.: Source and formation of secondary particulate matter in $PM_{2.5}$ in Asian continental outflow, J. Geophys. Res.-Atmos., 117, D03302, doi:10.1029/2011jd016400, 2012.

Fountoukis, C. and Nenes, A.: ISORROPIA II: a computationally efficient thermodynamic equilibrium model for K^+–Ca^{2+}–Mg^{2+}–NH_4^+–Na^+–SO_4^{2-}–NO_3^-–Cl^-–H_2O aerosols, Atmos. Chem. Phys., 7, 4639–4659, doi:10.5194/acp-7-4639-2007, 2007.

Fountoukis, C., Nenes, A., Sullivan, A., Weber, R., Van Reken, T., Fischer, M., Matías, E., Moya, M., Farmer, D., and Cohen, R. C.: Thermodynamic characterization of Mexico City aerosol during MILAGRO 2006, Atmos. Chem. Phys., 9, 2141–2156, doi:10.5194/acp-9-2141-2009, 2009.

Fridlind, A. M. and Jacobson, M. Z.: A study of gas-aerosol equilibrium and aerosol pH in the remote marine boundary layer during the First Aerosol Characterization Experiment (ACE 1), J. Geophys. Res.-Atmos., 105, 17325–17340, doi:10.1029/2000jd900209, 2000.

Froyd, K. D., Murphy, S. M., Murphy, D. M., de Gouw, J. A., Eddingsaas, N. C., and Wennberg, P. O.: Contribution of isoprene-derived organosulfates to free tropospheric aerosol mass, P. Natl. Acad. Sci. USA, 107, 21360–21365, doi:10.1073/pnas.1012561107, 2010.

Gaston, C. J., Riedel, T. P., Zhang, Z., Gold, A., Surratt, J. D., and Thornton, J. A.: Reactive Uptake of an Isoprene-derived Epoxydiol to Submicron Aerosol Particles, Environ. Sci. Technol., 48, 11178–11186, doi:10.1021/es5034266, 2014.

Guo, H., Xu, L., Bougiatioti, A., Cerully, K. M., Capps, S. L., Hite, J. R., Carlton, A. G., Lee, S.-H., Bergin, M. H., Ng, N. L., Nenes, A., and Weber, R. J.: Particle water and pH in the southeastern United States, Atmos. Chem. Phys. Discuss., 14, 27143–27193, doi:10.5194/acpd-14-27143-2014, 2014.

Gwynn, R. C., Burnett, R. T., and Thurston, G. D.: A time-series analysis of acidic particulate matter and daily mortality and morbidity in the Buffalo, New York, region, Environ. Health Persp., 108, 125–133, doi:10.2307/3454510, 2000.

Harris, D. C.: Quantitative Chemical Analysis, 5th Ed., edited by: Freeman, W. H. and Company, New York, 1999.

He, K., Zhao, Q., Ma, Y., Duan, F., Yang, F., Shi, Z., and Chen, G.: Spatial and seasonal variability of PM$_{2.5}$ acidity at two Chinese megacities: insights into the formation of secondary inorganic aerosols, Atmos. Chem. Phys., 12, 1377–1395, doi:10.5194/acp-12-1377-2012, 2012.

Hennigan, C. J., Sullivan, A. P., Fountoukis, C. I., Nenes, A., Hecobian, A., Vargas, O., Peltier, R. E., Case Hanks, A. T., Huey, L. G., Lefer, B. L., Russell, A. G., and Weber, R. J.: On the volatility and production mechanisms of newly formed nitrate and water soluble organic aerosol in Mexico City, Atmos. Chem. Phys., 8, 3761–3768, doi:10.5194/acp-8-3761-2008, 2008.

Huang, Y., Li, L., Li, J., Wang, X., Chen, H., Chen, J., Yang, X., Gross, D. S., Wang, H., Qiao, L., and Chen, C.: A case study of the highly time-resolved evolution of aerosol chemical and optical properties in urban Shanghai, China, Atmos. Chem. Phys., 13, 3931–3944, doi:10.5194/acp-13-3931-2013, 2013.

Jacobson, M. Z.: Studying the effects of calcium and magnesium on size-distributed nitrate and ammonium with EQUISOLV II, Atmos. Environ., 33, 3635–3649, doi:10.1016/S1352-2310(99)00105-3, 1999.

Jang, M., Cao, G., and Paul, J.: Colorimetric particle acidity analysis of secondary organic aerosol coating on submicron acidic aerosols, Aerosol. Sci. Tech., 42, 409–420, doi:10.1080/02786820802154861, 2008.

Johnson, A. H., Moyer, A., Bedison, J. E., Richter, S. L., and Willig, S. A.: Seven Decades of Calcium Depletion in Organic Horizons of Adirondack Forest Soils, Soil Sci. Soc. Am. J., 72, 1824–1830, doi:10.2136/sssaj2006.0407, 2008.

Keene, W. C. and Savoie, D. L.: The pH of deliquesced sea-salt aerosol in polluted marine air, Geophys. Res. Lett., 25, 2181–2184, doi:10.1029/98gl01591, 1998.

Keene, W. C., Sander, R., Pszenny, A. A. P., Vogt, R., Crutzen, P. J., and Galloway, J. N.: Aerosol pH in the marine boundary layer: A review and model evaluation, J. Aerosol Sci., 29, 339–356, doi:10.1016/S0021-8502(97)10011-8, 1998.

Keene, W. C., Pszenny, A. A. P., Maben, J. R., and Sander, R.: Variation of marine aerosol acidity with particle size, Geophys. Res. Lett., 29, 1101, doi:10.1029/2001gl013881, 2002.

Keene, W. C., Pszenny, A. A. P., Maben, J. R., Stevenson, E., and Wall, A.: Closure evaluation of size-resolved aerosol pH in the New England coastal atmosphere during summer, J. Geophys. Res.-Atmos., 109, D23307, doi:10.1029/2004jd004801, 2004.

Kerminen, V. M., Hillamo, R., Teinila, K., Pakkanen, T., Allegrini, I., and Sparapani, R.: Ion balances of size-resolved tropospheric aerosol samples: implications for the acidity and atmospheric processing of aerosols, Atmos. Environ., 35, 5255–5265, doi:10.1016/S1352-2310(01)00345-4, 2001.

Khlystov, A., Stanier, C. O., Takahama, S., and Pandis, S. N.: Water content of ambient aerosol during the Pittsburgh air quality study, J. Geophys. Res.-Atmos., 110, D07s10, doi:10.1029/2004jd004651, 2005.

Kim, Y. P., Seinfeld, J. H., and Saxena, P.: Atmospheric Gas Aerosol Equilibrium 1. Thermodynamic Model, Aerosol. Sci. Tech., 19, 157–181, doi:10.1080/02786829308959628, 1993.

Koutrakis, P., Wolfson, J. M., and Spengler, J. D.: An Improved Method for Measuring Aerosol Strong Acidity: Results from a Nine-month Study in St. Louis, Missouri and Kingston, Tennessee, Atmos. Environ., 22, 157–162, 1988.

Lawrence, J. and Koutrakis, P.: Measurement and speciation of gas and particulate phase organic acidity in an urban environment: 2. Speciation, J. Geophys. Res.-Atmos., 101, 9171–9184, doi:10.1029/95jd03357, 1996.

Likens, G. E., Driscoll, C. T., and Buso, D. C.: Long-term effects of acid rain: Response and recovery of a forest ecosystem, Science, 272, 244–246, doi:10.1126/science.272.5259.244, 1996.

Mahowald, N.: Aerosol Indirect Effect on Biogeochemical Cycles and Climate, Science, 334, 794–796, doi:10.1126/science.1207374, 2011.

Meng, Z. Y. and Seinfeld, J. H.: Time scales to achieve atmospheric gas-aerosol equilibrium for volatile species, Atmos. Environ., 30, 2889–2900, doi:10.1016/1352-2310(95)00493-9, 1996.

Meskhidze, N., Chameides, W. L., Nenes, A., and Chen, G.: Iron mobilization in mineral dust: Can anthropogenic SO$_2$ emissions affect ocean productivity?, Geophys. Res. Lett., 30, 2085, doi:10.1029/2003gl018035, 2003.

Meskhidze, N., Chameides, W. L., and Nenes, A.: Dust and pollution: A recipe for enhanced ocean fertilization?, J. Geophys. Res.-Atmos., 110, D03301, doi:10.1029/2004jd005082, 2005.

Metzger, S., Mihalopoulos, N., and Lelieveld, J.: Importance of mineral cations and organics in gas-aerosol partitioning of reactive nitrogen compounds: case study based on MINOS results, Atmos. Chem. Phys., 6, 2549–2567, doi:10.5194/acp-6-2549-2006, 2006.

Molina, L. T., Madronich, S., Gaffney, J. S., Apel, E., de Foy, B., Fast, J., Ferrare, R., Herndon, S., Jimenez, J. L., Lamb, B., Osornio-Vargas, A. R., Russell, P., Schauer, J. J., Stevens, P. S., Volkamer, R., and Zavala, M.: An overview of the MILAGRO 2006 Campaign: Mexico City emissions and their transport and transformation, Atmos. Chem. Phys., 10, 8697–8760, doi:10.5194/acp-10-8697-2010, 2010.

Moya, M., Pandis, S. N., and Jacobson, M. Z.: Is the size distribution of urban aerosols determined by thermodynamic equilibrium? An application to Southern California, Atmos. Environ., 36, 2349–2365, doi:10.1016/S1352-2310(01)00549-0, 2002.

Nenes, A., Pandis, S. N., and Pilinis, C.: ISORROPIA: A new thermodynamic equilibrium model for multiphase multicomponent inorganic aerosols, Aquat. Geochem., 4, 123–152, doi:10.1023/a:1009604003981, 1998.

Nenes, A., Pandis, S. N., and Pilinis, C.: Continued development and testing of a new thermodynamic aerosol module for urban and regional air quality models, Atmos. Environ., 33, 1553–1560, doi:10.1016/S1352-2310(98)00352-5, 1999.

Nenes, A., Krom, M. D., Mihalopoulos, N., Van Cappellen, P., Shi, Z., Bougiatioti, A., Zarmpas, P., and Herut, B.: Atmospheric acidification of mineral aerosols: a source of bioavailable phosphorus for the oceans, Atmos. Chem. Phys., 11, 6265–6272, doi:10.5194/acp-11-6265-2011, 2011.

Nguyen, Q. T., Christensen, M. K., Cozzi, F., Zare, A., Hansen, A. M. K., Kristensen, K., Tulinius, T. E., Madsen, H. H., Christensen, J. H., Brandt, J., Massling, A., Nøjgaard, J. K., and Glasius, M.: Understanding the anthropogenic influence on formation of biogenic secondary organic aerosols in Denmark via analysis of organosulfates and related oxidation products, Atmos. Chem. Phys., 14, 8961–8981, doi:10.5194/acp-14-8961-2014, 2014.

Paciga, A. L., Riipinen, I., and Pandis, S. N.: Effect of Ammonia on the Volatility of Organic Diacids, Environ. Sci. Technol., 48, 13769–13775, doi:10.1021/es5037805, 2014.

Pan, Y. P., Wang, Y. S., Tang, G. Q., and Wu, D.: Spatial distribution and temporal variations of atmospheric sulfur deposition in Northern China: insights into the potential acidification risks, Atmos. Chem. Phys., 13, 1675–1688, doi:10.5194/acp-13-1675-2013, 2013.

Pathak, R. K., Yao, X. H., and Chan, C. K.: Sampling artifacts of acidity and ionic species in $PM_{2.5}$, Environ. Sci. Technol., 38, 254–259, doi:10.1021/Es0342244, 2004.

Pathak, R. K., Wu, W. S., and Wang, T.: Summertime $PM_{2.5}$ ionic species in four major cities of China: nitrate formation in an ammonia-deficient atmosphere, Atmos. Chem. Phys., 9, 1711–1722, doi:10.5194/acp-9-1711-2009, 2009.

Pathak, R. K., Wang, T., Ho, K. F., and Lee, S. C.: Characteristics of summertime $PM_{2.5}$ organic and elemental carbon in four major Chinese cities: Implications of high acidity for water-soluble organic carbon (WSOC), Atmos. Environ., 45, 318–325, doi:10.1016/j.atmosenv.2010.10.021, 2011.

Peltier, R. E., Sullivan, A. P., Weber, R. J., Wollny, A. G., Holloway, J. S., Brock, C. A., de Gouw, J. A., and Atlas, E. L.: No evidence for acid-catalyzed secondary organic aerosol formation in power plant plumes over metropolitan Atlanta, Georgia, Geophys. Res. Lett., 34, L06801, doi:10.1029/2006gl028780, 2007.

Pilinis, C. and Seinfeld, J. H.: Continued development of a general equilibrium model for inorganic multicomponent atmospheric aerosols, Atmos. Environ., 21, 2453–2466, doi:10.1016/0004-6981(87)90380-5, 1987.

Pszenny, A. A. P., Moldanová, J., Keene, W. C., Sander, R., Maben, J. R., Martinez, M., Crutzen, P. J., Perner, D., and Prinn, R. G.: Halogen cycling and aerosol pH in the Hawaiian marine boundary layer, Atmos. Chem. Phys., 4, 147–168, doi:10.5194/acp-4-147-2004, 2004.

Reid, J. S., Hobbs, P. V., Ferek, R. J., Blake, D. R., Martins, J. V., Dunlap, M. R., and Liousse, C.: Physical, chemical, and optical properties of regional hazes dominated by smoke in Brazil, J. Geophys. Res.-Atmos., 103, 32059–32080, doi:10.1029/98jd00458, 1998.

Sander, R. and Crutzen, P. J.: Model study indicating halogen activation and ozone destruction in polluted air masses transported to the sea, J. Geophys. Res.-Atmos., 101, 9121–9138, doi:10.1029/95jd03793, 1996.

Schindler, D. W.: Effects of Acid-Rain on Fresh-Water Ecosystems, Science, 239, 149–157, doi:10.1126/science.239.4836.149, 1988.

Stoddard, J. L., Jeffries, D. S., Lukewille, A., Clair, T. A., Dillon, P. J., Driscoll, C. T., Forsius, M., Johannessen, M., Kahl, J. S., Kellogg, J. H., Kemp, A., Mannio, J., Monteith, D. T., Murdoch, P. S., Patrick, S., Rebsdorf, A., Skjelkvale, B. L., Stainton, M. P., Traaen, T., van Dam, H., Webster, K. E., Wieting, J., and Wilander, A.: Regional trends in aquatic recovery from acidification in North America and Europe, Nature, 401, 575–578, doi:10.1038/44114, 1999.

Stumm, W. and Morgan, J. J.: Aquatic chemistry : chemical equilibria and rates in natural waters, Wiley, New York, 1996.

Sun, Y.-L., Zhang, Q., Schwab, J. J., Demerjian, K. L., Chen, W.-N., Bae, M.-S., Hung, H.-M., Hogrefe, O., Frank, B., Rattigan, O. V., and Lin, Y.-C.: Characterization of the sources and pro-

cesses of organic and inorganic aerosols in New York city with a high-resolution time-of-flight aerosol mass apectrometer, Atmos. Chem. Phys., 11, 1581–1602, doi:10.5194/acp-11-1581-2011, 2011.

Surratt, J. D., Lewandowski, M., Offenberg, J. H., Jaoui, M., Kleindienst, T. E., Edney, E. O., and Seinfeld, J. H.: Effect of acidity on secondary organic aerosol formation from isoprene, Environ. Sci. Technol., 41, 5363–5369, doi:10.1021/Es0704176, 2007.

Takahama, S., Davidson, C. I., and Pandis, S. N.: Semicontinuous measurements of organic carbon and acidity during the Pittsburgh air quality study: Implications for acid-catalyzed organic aerosol formation, Environ. Sci. Technol., 40, 2191–2199, doi:10.1021/Es050856+, 2006.

Tanner, R. L., Olszyna, K. J., Edgerton, E. S., Knipping, E., and Shaw, S. L.: Searching for evidence of acid-catalyzed enhancement of secondary organic aerosol formation using ambient aerosol data, Atmos. Environ., 43, 3440–3444, doi:10.1016/j.atmosenv.2009.03.045, 2009.

Thornton, J. A., Kercher, J. P., Riedel, T. P., Wagner, N. L., Cozic, J., Holloway, J. S., Dube, W. P., Wolfe, G. M., Quinn, P. K., Middlebrook, A. M., Alexander, B., and Brown, S. S.: A large atomic chlorine source inferred from mid-continental reactive nitrogen chemistry, Nature, 464, 271–274, doi:10.1038/Nature08905, 2010.

Trebs, I., Metzger, S., Meixner, F. X., Helas, G. N., Hoffer, A., Rudich, Y., Falkovich, A. H., Moura, M. A. L., da Silva, R. S., Artaxo, P., Slanina, J., and Andreae, M. O.: The NH_4^+-NO_3^--Cl^--SO_4^{2-}-H_2O aerosol system and its gas phase precursors at a pasture site in the Amazon Basin: How relevant are mineral cations and soluble organic acids?, J. Geophys. Res.-Atmos., 110, D07303, doi:10.1029/2004jd005478, 2005.

Wexler, A. S. and Clegg, S. L.: Atmospheric aerosol models for systems including the ions H^+, NH_4^+, Na^+, SO_4^{2-}, NO_3^-, Cl^-, Br^-, and H_2O, J. Geophys. Res.-Atmos., 107, 4207, doi:10.1029/2001jd000451, 2002.

Winkler, P.: Relations Between Aerosol Acidity and Ion Balance, in: Chemistry of Multiphase Atmospheric Systems, edited by: Jaeschke, W., 6, Springer-Verlag, New York, 269–298, 1986.

Xu, L., Guo, H., Boyd, C. M., Klein, M., Bougiatioti, A., Cerully, K. M., Hite, J. R., Isaacman-VanWertz, G., Kreisberg, N. M., Knote, C., Olson, K., Koss, A., Goldstein, A. H., Hering, S. V., de Gouw, J., Baumann, K., Lee, S.-H., Nenes, A., Weber, R. J., and Ng, N. L.: Effects of anthropogenic emissions on aerosol formation from isoprene and monoterpenes in the southeastern United States, P. Natl. Acad. Sci. USA, 112, 37–42, doi:10.1073/pnas.1417609112, 2015.

Yao, X. H., Ling, T. Y., Fang, M., and Chan, C. K.: Comparison of thermodynamic predictions for in situ pH in $PM_{2.5}$, Atmos. Environ., 40, 2835–2844, doi:10.1016/j.atmosenv.2006.01.006, 2006.

Young, A. H., Keene, W. C., Pszenny, A. A. P., Sander, R., Thornton, J. A., Riedel, T. P., and Maben, J. R.: Phase partitioning of soluble trace gases with size-resolved aerosols in near-surface continental air over northern Colorado, USA, during winter, J. Geophys. Res.-Atmos., 118, 9414–9427, doi:10.1002/Jgrd.50655, 2013.

Zaveri, R. A., Easter, R. C., Fast, J. D., and Peters, L. K.: Model for Simulating Aerosol Interactions and Chemistry (MOSAIC), J. Geophys. Res.-Atmos., 113, D13204, doi:10.1029/2007jd008782, 2008.

Zhang, H. F., Worton, D. R., Lewandowski, M., Ortega, J., Rubitschun, C. L., Park, J. H., Kristensen, K., Campuzano-Jost, P., Day, D. A., Jimenez, J. L., Jaoui, M., Offenberg, J. H., Kleindienst, T. E., Gilman, J., Kuster, W. C., de Gouw, J., Park, C., Schade, G. W., Frossard, A. A., Russell, L., Kaser, L., Jud, W., Hansel, A., Cappellin, L., Karl, T., Glasius, M., Guenther, A., Goldstein, A. H., Seinfeld, J. H., Gold, A., Kamens, R. M., and Surratt, J. D.: Organosulfates as Tracers for Secondary Organic Aerosol (SOA) Formation from 2-Methyl-3-Buten-2-ol (MBO) in the Atmosphere, Environ. Sci. Technol., 46, 9437–9446, doi:10.1021/Es301648z, 2012a.

Zhang, Q., Jimenez, J. L., Worsnop, D. R., and Canagaratna, M.: A case study of urban particle acidity and its influence on secondary organic aerosol, Environ. Sci. Technol., 41, 3213–3219, doi:10.1021/Es061812j, 2007.

Zhang, X., Liu, Z., Hecobian, A., Zheng, M., Frank, N. H., Edgerton, E. S., and Weber, R. J.: Spatial and seasonal variations of fine particle water-soluble organic carbon (WSOC) over the southeastern United States: implications for secondary organic aerosol formation, Atmos. Chem. Phys., 12, 6593–6607, doi:10.5194/acp-12-6593-2012, 2012b.

Zhang, Y., Seigneur, C., Seinfeld, J. H., Jacobson, M., Clegg, S. L., and Binkowski, F. S.: A comparative review of inorganic aerosol thermodynamic equilibrium modules: similarities, differences, and their likely causes, Atmos. Environ., 34, 117–137, doi:10.1016/S1352-2310(99)00236-8, 2000.

Ziemba, L. D., Fischer, E., Griffin, R. J., and Talbot, R. W.: Aerosol acidity in rural New England: Temporal trends and source region analysis, J. Geophys. Res.-Atmos., 112, D10s22, doi:10.1029/2006jd007605, 2007.